



Theoretical analysis of Poiseuille flow instabilities in nematics

P. Manneville

► To cite this version:

P. Manneville. Theoretical analysis of Poiseuille flow instabilities in nematics. *Journal de Physique*, 1979, 40 (7), pp.713-724. 10.1051/jphys:01979004007071300 . jpa-00209156

HAL Id: jpa-00209156

<https://hal.science/jpa-00209156>

Submitted on 4 Feb 2008

HAL is a multi-disciplinary open access archive for the deposit and dissemination of scientific research documents, whether they are published or not. The documents may come from teaching and research institutions in France or abroad, or from public or private research centers.

L'archive ouverte pluridisciplinaire **HAL**, est destinée au dépôt et à la diffusion de documents scientifiques de niveau recherche, publiés ou non, émanant des établissements d'enseignement et de recherche français ou étrangers, des laboratoires publics ou privés.

Classification
Physics Abstracts
47.15F

Theoretical analysis of Poiseuille flow instabilities in nematics

P. Manneville

Service de Physique du Solide et de Résonance Magnétique,
Orme des Merisiers, B.P. n° 2, 91190 Gif sur Yvette, France

(Reçu le 19 décembre 1978, accepté le 5 mars 1979)

Résumé. — Nous étudions la stabilité de l'écoulement de Poiseuille dans un nématique en géométrie planaire. Nous prolongeons l'analyse de la référence [5] pour tenir compte des distorsions périodiques du directeur. Plusieurs approches différentes sont mises en œuvre : modèles simplifiés, méthode de Galerkin ou simulation numérique. Nos résultats permettent d'interpréter l'ensemble des données expérimentales obtenues jusqu'à présent (réfs. [4] et [9]).

Abstract. — We study the stability of a Poiseuille flow in a planar nematic. We extend the analysis given in ref. [5] to take into account periodic distortions of the director. Several different approaches are employed : simplified models, Galerkin method, or numerical simulation. Our results allow one to interpret experimental findings so far obtained (refs. [4] and [9]).

1. Introduction. — Recently much attention has been devoted to hydrodynamic instabilities in Nematic Liquid Crystals [1]. A situation of particular interest is achieved when the mean molecular orientation is perpendicular to the shearing plane [2]. Instabilities which set in then result from the very specific coupling between the velocity field and the director ; they occur at very low Reynolds numbers. The case of the Simple Shear Flow (S.S.F. in the following) is pretty well understood [3]. Steady as well as alternating flows have been investigated and the effects of applied electric and magnetic fields have been examined. Two different instability modes can take place : a uniform distortion called the Homogeneous Instability (H.I.) and a periodic distortion, the Roll Instability (R.I.). Essential parameters are the sign of α_3 , the intensity of the external fields and/or the frequency. When $\alpha_3 > 0$ only the R.I. can take place. When $\alpha_3 < 0$, the H.I. which sets in at low field/frequency is replaced by the R.I. at high field/frequency. Quantitative agreement between experiments and theory is quite satisfactory.

Before a complete understanding of the S.S.F. instabilities was obtained, planar Poiseuille flow began to be investigated. The first experimental results were qualitatively accounted for by a model in terms of an assemblage of average simple shear flows [4] but the detailed theoretical analysis turned

out to be far more difficult. First results obtained concerned the symmetry properties of the unstable modes (which lead to a useful classification of experimental facts) and the detailed solution of the steady flow H.I. [5] in complete agreement with experiments. However experiments revealed more complexities than one could have inferred from the simple transposition of the simple shear flow case and much remained to be accounted for.

In this paper we intend to complete the theoretical account of experiments. The main source of difficulty originates from the fact that the shearing rate of the primary flow is no longer constant so that some coefficients of the partial differential equations governing the problem become variable. To cope with this difficulty we shall develop essentially three different kinds of approach : approximate models, Galerkin analysis or direct numerical integration. Detailed calculations are rather lengthy and tedious, so they will be skipped over since they have been reported elsewhere [6]. Notations and general equations have already been given [7] and will not be repeated here. The paper is organized as follows :

— In section 2, we recall the symmetry of the unstable modes and the solution of the steady flow Homogeneous Instability. We take advantage of its simplicity to check the prototype of approximate models to be used in other sections.

— Section 3 is devoted to the effect of external fields on homogeneous as well as periodic instability modes.

— Then the analysis is extended to alternating flows (§ 4). Specific features of the stability analysis and additional symmetry properties are briefly discussed. Then we consider the alternating Homogeneous Instability which is solved by direct numerical integration. The case of rolls is discussed within the framework of an approximate model derived from that presented in § 2.

— Finally, agreement between experiments and theory is examined in section 5, and prospects for future work are suggested.

Now, before we begin by recalling previous results, let us briefly present the experimental situation. The geometry of the set-up is sketched in figure 1. The channel has length L , width l and height d . The fluid is submitted to a pressure drop Δp corresponding to a pressure gradient $G_y = \Delta p/L$. Through surface treatment, the nematic is oriented parallel to the direction of the width. As long as G_y is small enough, the director \mathbf{n} remains everywhere perpendicular to the shearing plane and the velocity assumes the usual parabolic profile

$$v_y^0 = \frac{|G_y|}{2\eta_3} \left(\frac{d}{2}\right)^2 \left[1 - \left(\frac{2z}{d}\right)^2\right]$$

which leads to the z -dependent shearing rate

$$s(z) = \partial_z v_y^0 = -|G_y|z/\eta_3$$

and this proves to be the main source of difficulties for the theoretical analysis. When G_y exceeds a critical value, the orientation gets distorted and secondary flows set in. From an experimental point of view, the instability is linear ⁽¹⁾ and stationary ⁽²⁾ [8].

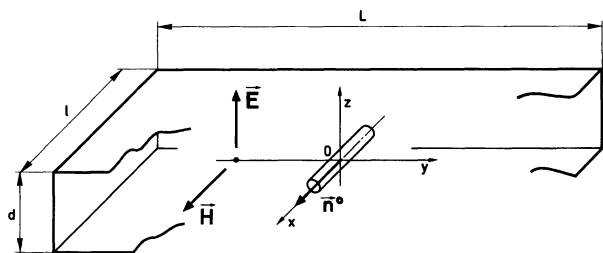


Fig. 1. — A pressure gradient $G_y = \Delta p/L$ is applied between the two ends of a channel of rectangular section. Upper and lower plates have received a special treatment so that the anchoring of the nematic molecules is planar and parallel to the x -axis. The nematic may be submitted to a magnetic field $H(\parallel Ox)$ and/or an electrical field $E(\parallel Oz)$. Origin of coordinates is taken at the centre of the channel.

⁽¹⁾ With the exception of the so-called Z-regime which develops in alternating flow under high electric field [9].

⁽²⁾ In the linear regime, the distortion growth is exponential, the growth rate σ is real and $\sigma = 0_+$ corresponds to the threshold (marginal case); for alternating flows, see the extension of the meaning discussed at the beginning of section 3.

2. **Summary of previous results** [5]. — From the linearized equations which govern an infinitesimal perturbation $(n_y, n_z, v_x, v_y, v_z, p)$ to the primary flow [7], recalling that $s(-z) = -s(z)$, one can classify the unstable modes according to their parity (table I).

Table I. — *Parity properties of the unstable modes.*

	n_y	n_z	v_x	v_y	v_z	p
T	even	odd	even	even	odd	even
S	odd	even	odd	odd	even	odd

Solution T (resp. S) is associated with an average finite Twist (resp. Splay) distortion :

$$T \text{ (resp. S)} = \frac{1}{d} \times \int_{-d/2}^{d/2} dz n_y(z) \text{ (resp. } n_z(z)) \neq 0 \text{ (in general) ;}$$

parity properties of v_x will turn out to be very important. These formal symmetry properties were already underlying the first qualitative analysis of the flow in terms of the juxtaposition of two average opposite simple shearflows [4]. However such a point of view only leads to rough estimates of the threshold properties and a complete analysis had to take into account the spatial variation of the shearing rate. The first step in this direction was the analysis of the steady flow Homogeneous Instability for a nematic with $\alpha_3 < 0$ [5]. In absence of external field a complete analytical solution can be derived. The threshold is given by $Er^c = 12.824$ where the Ericksen number Er is the relevant dimensionless measure of the flow gradient

$$\left(\text{here } Er = \frac{|G_y|}{\eta_3} \left(\frac{d}{2}\right)^3 \sqrt{\frac{\alpha_2 \alpha_3}{K_1 K_2} \frac{\eta_3}{\eta_1}}\right).$$

The corresponding unstable mode is a T-solution with net transverse flow

$$\left(V_x = \frac{1}{d} \int_{-d/2}^{d/2} dz v_x(z) \neq 0\right).$$

In presence of external fields the possibility of an analytical solution is lost in general, due to the anisotropy of the Frank elastic constants. However an approximate numerical Galerkin type analysis (Chandrasekhar's method [8]) has shown that this anisotropy is of little importance and that results are close to what is obtained in the ideal case of isotropic elasticity (for which the analytical approach remains tractable). The intensity of a stabilizing external magnetic field applied parallel to the unperturbed orientation can be measured by

$$F = \left(\frac{d}{2}\right)^2 \chi_a H^2 / \bar{K}$$

which expresses the ratio of the magnetic torque to the elastic one (\bar{K} is some average value for the Frank constant). The variation of the threshold with the field is given by

$$F = Er^c - 2.388(Er^c)^{2/3}. \quad (1)$$

Contrary to what was first thought, such a peculiar variation can in fact easily be derived from a simplified model that we shall develop here, since we shall refer to it in section 3 and 4. Let us consider figure 2a which presents the fluctuation profile of the T-distortion at high fields ($F = 150$). In the central part ($z \sim 0$) where the shearing rate is small, the distortion is small due to the stabilizing effect of the field. On the contrary in the neighbourhood of the plates ($z \sim \pm d/2$) the Pieranski-Guyon instability mechanism leads to a large distortion. This strongly suggests the simplified distortion depicted on figure 2b where a stable central layer is assumed to separate unstable layers of thickness δ ($0 < \delta \ll d/2$) close to the plates. The distortion is taken of the form

$$n_\alpha \propto \pm \sin\left(\frac{\pi}{\delta} \xi\right) \quad (\alpha = y \text{ or } z)$$

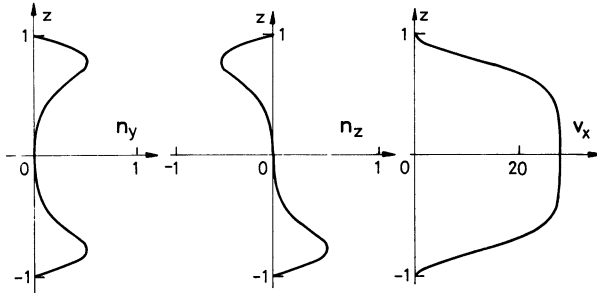


Fig. 2a. — Solution of the exact calculation : in the central region the distortion is very small due to the stabilizing effect of the field while the destabilizing mechanism proportional to the square of the shearing rate is very weak.

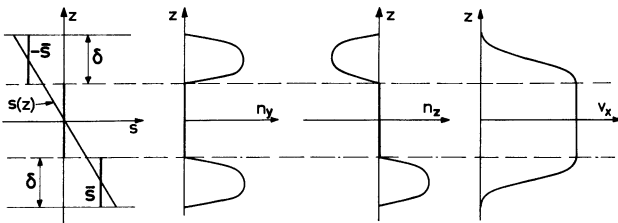


Fig. 2b. — Approximate model describing the situation of figure 2a : two unstable layers of thickness δ are submitted to an average simple shear $\pm \bar{s}(\delta)$. Optimizing δ leads to an excellent agreement with the exact calculation.

Fig. 2. — Fluctuation profiles under large fields (here $F = \chi_a H^2 d^2 / 4 K \sim 150$) for the homogeneous instability discussed in ref. [5].

where ξ represents the distance to the plate, and the unstable layers are submitted to an average shear

$$\bar{s} = \frac{1}{\delta} \int_0^\delta s(\xi) d\xi = \frac{|G_y|}{2\eta_3} (d - \delta) = \bar{s}(\delta).$$

The instability criterion is then given by the Simple Shear flow theory [7]

$$\bar{s}^2 \alpha_2 \alpha_3 \frac{\eta_3}{\eta_1} = \left[\bar{K} \left(\frac{\pi}{\delta} \right)^2 + \chi_a H^2 \right]^2 \quad (2)$$

in which δ is still a free parameter. The threshold is then given by the value δ_c which minimizes the critical shear. Turning to dimensionless notations, with $\Delta = 2\delta/d$ one gets (2) in the form

$$Er(1 - \Delta/2) = (\pi^2/\Delta^2 + F). \quad (2')$$

The extremum condition $\partial Er/\partial \Delta = 0$ reads

$$\Delta^3 F + 3\pi^2 \Delta - 4\pi^2 = 0 \quad (3)$$

and when F is large the root of eq. (3) is approximately given by

$$\Delta_c = (4\pi^2/F)^{1/3} \quad (3')$$

so that

$$Er^c \simeq F + \left[\frac{\pi^2}{(4\pi^2)^{2/3}} + \frac{(4\pi^2)^{1/3}}{2} \right] F^{2/3} + o(F^{1/3}) = F + 2.55 F^{2/3} + o(F^{1/3})$$

in excellent agreement with the analytical result (1) which we can write $Er^c = F + 2.388 F^{2/3} + o(F^{1/3})$.

Let us take the opportunity to stress the fact that Δ (or δ) is *not* a coherence length as it is defined for example in the Fredericks problem [10]. In that case the coherence length is directly related to the balance between the magnetic torque and the elastic one when surface effects and field effects are conflicting : this leads to $\delta \sim 1/H$. In the present case, these effects are not conflicting but both struggle with the destabilizing mechanism, which leads to a more involved compromise and to the rather strange dependence $\delta \sim H^{-2/3}$: a simple dimensional argument based on the *Fredericks coherence length* (irrelevant to the present problem) would fail.

3. Steady Poiseuille flow : general approach. — In the simple shear flow case the uniform distortion corresponding to the Homogeneous Instability can take place at low fields when α_3 is negative. At higher fields a distortion sets in which is periodic in the direction of the unperturbed orientation, this distortion is associated with a secondary flow in form of rolls, the order of magnitude of the wavelength being given by the thickness of the unstable layer. Recalling the analogy between a Poiseuille flow and two juxtaposed simple shear flows one expects

such a roll instability to be possible (Fig. 3) and one can estimate the cross-over field from the H.I. to the R.I. Even at fields much larger than this estimated cross-over field and at least for steady flows such a transition *has not* been observed experimentally which clearly needs an explanation. The origin of the discrepancy can be traced back to the coupling both elastic and viscous between the upper and lower halves of the channel which must alter the simple picture of Poiseuille flow in terms of *decoupled* unstable layers submitted to average simple shears. Unfortunately a quantitative account of this effect leads to a cumbersome analysis. The normal mode analysis developed for the simple shear case [7] no longer works due to the z -dependence of the shearing rate and one must turn to a Galerkin approach (Chandrasekhar's method [8]) derived from that outlined in ref. [5] for the Homogeneous Instability. Calculations result in the determination of the complete curve of marginal stability i.e. the critical pressure drop (or Ericksen number) as a function of the wave vector q_x of the periodic distortion.

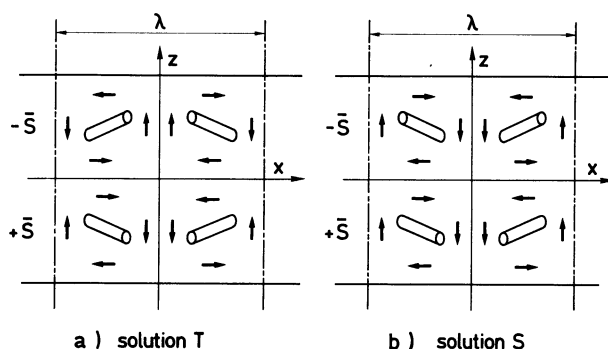


Fig. 3. — Qualitative picture of the rolls assuming the Poiseuille flow as the juxtaposition of two average simple shears and neglecting the coupling between the two halves of the channel. n_y is even and n_z is odd for a solution with average twist (T → figure 3a); on the contrary for a solution S, n_y is odd and so is v_x , which implies that the rolls do not gear properly (Fig. 3b).

The instability threshold corresponds to the absolute minimum of the curve. As in the case of the simple shear flow one expects the marginal stability curve to separate in two different regions : the one at small wave vectors ($q_x \ll 2\pi/d$) connected with the homogeneous instability, the other at larger wave vectors ($q_x \gtrsim 2\pi/d$) connected with rolls. T and S modes may be separated from the beginning and will be studied one after the other.

3.1 T-TYPE ROLL INSTABILITY. — T-distortion is associated with an average twist and with a fluctuation $n_y(z)$ which is an even function of z . Calculations parallel to those of ref. [5] have been performed assuming

$$n_y = \sum_{n=1}^{\infty} \left[A_n \cos \left(n - \frac{1}{2} \right) \pi z \right] \cos q_x x.$$

Numerical applications correspond to MBBA, the nematic which was used in experiments. The resulting marginal stability curve is given in figure 4 where we have plotted the Ericksen number, here

$$Er = \frac{|G_y|}{\eta_3} \left(\frac{d}{2} \right)^3 \sqrt{\frac{\alpha_2 \alpha_3}{K_1 K_2}},$$

as a function of the reduced wave vector $Q = q_x d/2$. Intensity of the external fields is measured by

$$F_y = \frac{\chi_a H^2}{K_2} \left(\frac{d}{2} \right)^2 \quad \text{and} \quad F_z = \frac{\chi_a H^2 - (\epsilon_a/4\pi) E^2}{K_1} \left(\frac{d}{2} \right)^2.$$

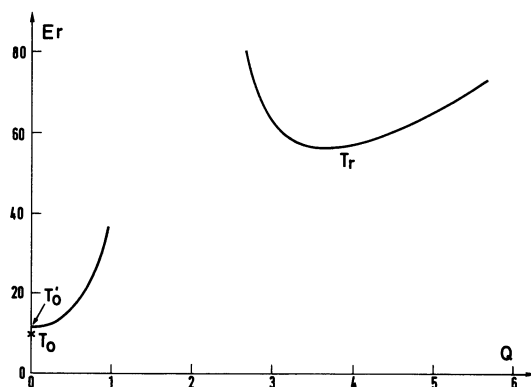


Fig. 4. — Critical curve for solution T. The Ericksen number

$$Er = \frac{|G_y|}{\eta_3} \left(\frac{d}{2} \right)^3 \sqrt{\frac{\alpha_2 \alpha_3}{K_1 K_2}}$$

is given as a function of the reduced wave vector $Q = q_x d/2$. Solution T_0 (resp. T'_0) corresponds to a homogeneous instability with (resp. without) net transverse flow (see Fig. 5). Solution T_r corresponds to rolls.

The curve presented corresponds to $F_y = F_z = 0$ (no external fields). As expected it is composed of two branches. Let us first consider the small q_x part. When q_x tends to zero, this branch presents a minimum denoted T'_0 slightly above the point T_0 obtained from the direct calculation with $q_x = 0$ (i.e. assuming from the very start a fluctuation independent of x , results were given in section 2 using a slightly different definition for the Ericksen number). This is not a spurious numerical result : T'_0 and T_0 must be associated with two different homogeneous instabilities. This can be understood from the comparison of the fluctuation profiles given in figure 5. For a T-type solution, the transverse velocity v_x is an even function of z , which does not forbid an average net transverse flow

$$V_x = \frac{1}{d} \int_{-d/2}^{d/2} v_x(z) dz \neq 0$$

and solution T_0 is indeed associated with such a transverse flow. On the contrary, solution T'_0 corres-

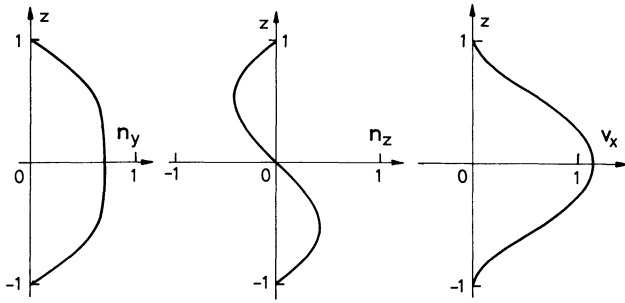


Fig. 5a. — Solution T_0 with net transverse flow ($\int v_x dz \neq 0$) as obtained in ref. [5] by a direct calculation assuming fluctuations independent of x (q_x strictly equal to zero).

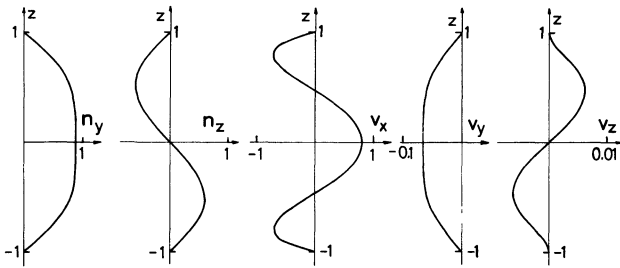


Fig. 5b. — Solution T'_0 without net transverse flow ($\int v_x dz = 0$) limit $q_x \rightarrow 0$ of a calculation assuming periodic fluctuations with wave vector q_x (at the limit $q_x \rightarrow 0$, v_y and v_z vanish; here $Q = q_x d/2 = 5 \times 10^{-2}$).

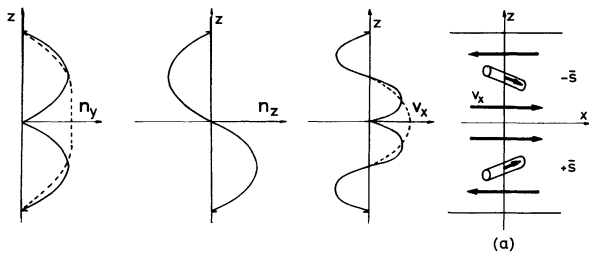


Fig. 5c. — Solution T'_0 emerges directly from the juxtaposition of two simple shear flow instabilities (full line) after relaxation of a part of the elastic energy contained in distortion n_y (dashed line).

Fig. 5. — Fluctuation profiles for the two homogeneous solutions T_0 and T'_0 .

ponds to $V_x = 0$; this could be expected since T'_0 is obtained at the limit $q_x \rightarrow 0$ of a calculation which assumes a strictly periodic fluctuation of wave vector $q_x \neq 0$ (without any component at $q_x = 0$). An integration of the continuity equation $\partial_x v_x + \partial_z v_z = 0$ over the height d of the channel then leads to :

$$q_x \int_{-d/2}^{d/2} v_x(z) dz \propto v_x \left(+\frac{d}{2} \right) - v_x \left(-\frac{d}{2} \right) = 0$$

from the velocity boundary conditions. This implies $q_x V_x = 0$ and $V_x = 0$ as long as $q_x \neq 0$ even at the

limit $q_x \rightarrow 0$ (except at $q_x = 0$ where one can have $V_x \neq 0$). That T_0 be an isolated point is then not a surprise. Solution T'_0 is in fact very close to what one would expect from the analogy between the Poiseuille flow and the two juxtaposed average simple shears (Fig. 5c). Profiles of the orientation fluctuations n_y and n_z are very similar for T_0 and T'_0 , which explains that the threshold values are nearly identical. The calculation shows that the most unstable mode is solution T_0 with transverse flow. This is in complete agreement with experimental results : Regime B of ref. [9] which occurred at threshold was associated with a transverse flow leading to a regular domain structure. Another regime denoted A, with average twist but without net transverse flow could also take place but was metastable and had a higher threshold. First velocity measurements are too incomplete to rule out the identification of regime A with our solution T'_0 and we urge a check of the two superposed wide rolls suggested on figure 5c.

The branch defined for $q_x \gtrsim 2\pi/d$ corresponds to a true roll instability : it presents a minimum denoted as T_r . Fluctuation profiles given in figure 6 are

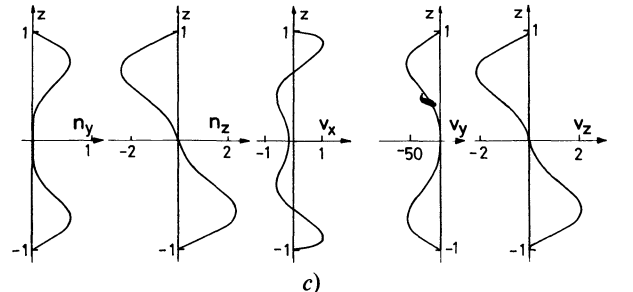
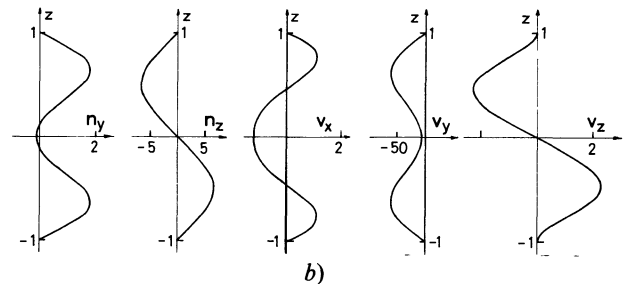
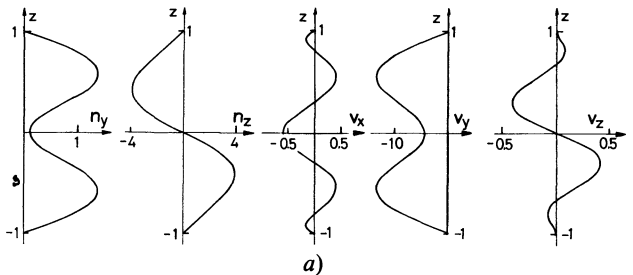


Fig. 6. — Fluctuation profiles for the roll solution T_r : figure 6, a, b, c correspond to different external fields measured by F_y and F_z (see text) (a) $F_y = F_z = F = 0$; (b) $F = 100$; (c) $F = 500$. Profiles are roughly as expected from the qualitative point of view illustrated in figure 3. When the fields are increased, a stable layer with small distortion tends to separate the cell in two decoupled parts.

roughly as expected from the naive sketch (Fig. 3a). Upper and lower halves of the channel are rather uncoupled and a stable layer appear in the central part ($z \sim 0$) with increasing fields. Evolution of the instability threshold with external fields is given in figure 7 for the three T-solutions. One can see that the homogeneous instability *with* transverse flow T_0 has always the lowest critical value and that if it did not exist one would observe the cross-over from T'_0 to T_r exactly as in the simple shear case.

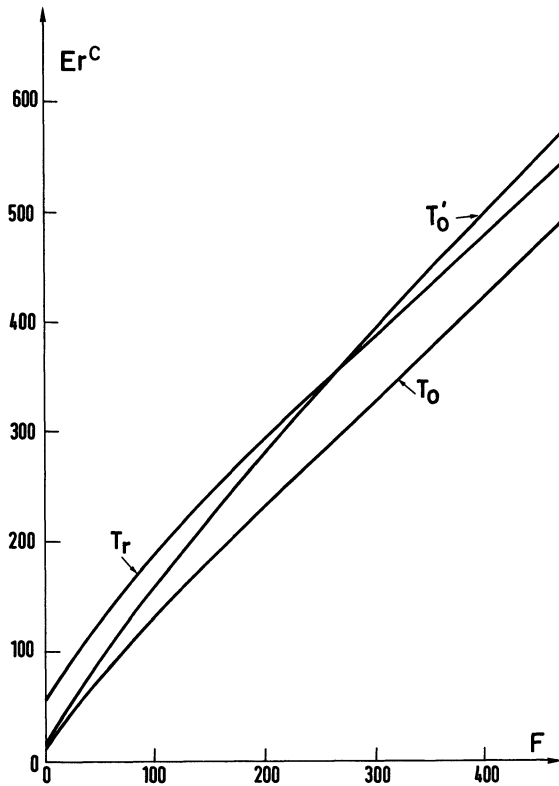


Fig. 7. — Threshold of the three different solutions with average twist as a function of external fields.

3.2 S-TYPE ROLL INSTABILITY. — A distortion with average splay corresponds to a fluctuation $n_y(z)$ which is an odd function of z , so that the calculation has been performed assuming

$$n_y = \sum_n [A_n \sin n\pi z] \cos q_x x.$$

Figure 9 displays marginal stability curves for several values of the external fields. The two branches at small and large q_x only appear for large enough external fields. This can be understood from the qualitative picture of figure 3b. Indeed an S-type solution involves an odd transverse velocity v_x and

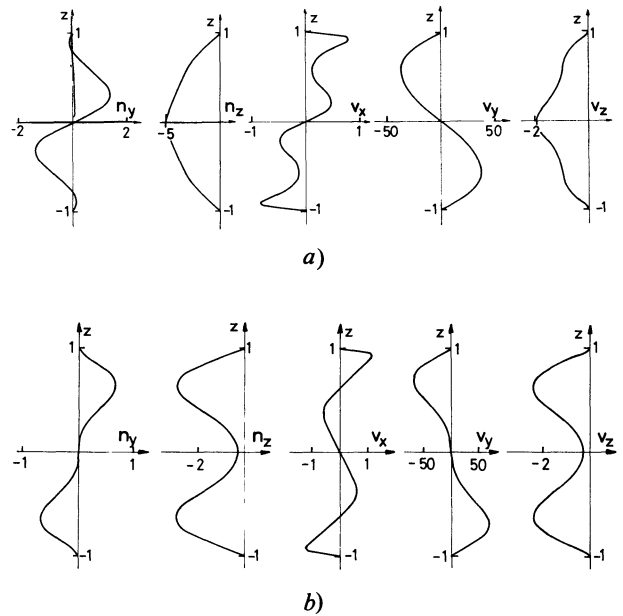


Fig. 9. — Fluctuation profiles for solution S_r ; (a) $F = 100$, the situation is still far from what was expected in figure 3b. (b) $F = 500$ the two halves of the channel are rather decoupled by the *stable* layer, distortions begin to concentrate close to the plate, apart from parity profiles look like those given in figure 6c for rolls T_r .

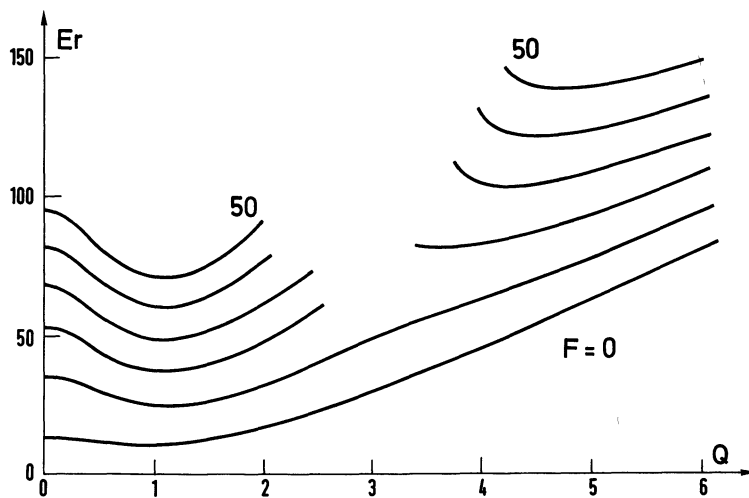


Fig. 8. — S-critical curves for different values of external fields. Rolls can take place only if F is large enough.

a strong velocity gradient $\partial_z v_x$ in the mid-plane ($z=0$); in other words, rolls do not gear correctly. Distortions in the upper and lower halves of the channel are so strongly coupled that a roll instability with a wave vector of the order of $2\pi/d$ cannot exist in zero field. With increasing field, the role of the central layer ($z \sim 0$) weakens and a roll instability can exist. At moderate fields, fluctuation profiles are still far from what one expects (Fig. 9a) but the situation gets better at higher fields and the two halves of the channel become uncoupled (Fig. 9b).

Let us now turn to the small q_x part of the curve. On the enlargement given in figure 10 for $F_y = F_z = 0$, one first notices that the minimum does not take place at $q_x = 0$ but rather at $Q = q_x d/2 \sim 1$ so that the homogeneous S-type instability studied in ref. [5] and denoted here as S_0 is in fact unstable against a roll fluctuation of long wavelength (since v_x is odd, the net transverse flow is zero and the discontinuity at $q_x = 0$ does not appear). Figure 11 displays the fluctuation profiles at S_0 and at the minimum of the curve. v_x and n_y are quite similar and the fact that S_0 lies slightly above the minimum is to be related to the shape of n_z . Indeed the dominant part of the elastic energy is $\frac{1}{2} K_1 \int (\partial_z n_z)^2 dz$ and when n_z gets more regular, this energy gets smaller and the instability threshold decreases. In the following we shall denote the minimum of the curve S'_0 to recall that it occurs at small wave vectors (index 0) and originates from the relaxation of a part of the elastic energy contained in solution S_0 . It should be noted here that calculations have been performed using values of the viscoelastic coefficients for MBBA tabulated in ref. [10] (with $\alpha_3/\alpha_2 = 1.53 \times 10^{-2}$);

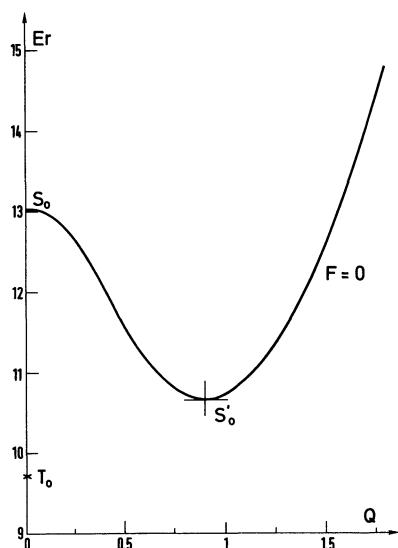


Fig. 10. — Enlargement of the small q_x part of the curve $F = 0$ given in figure 8. Solution S_0 discussed in ref. [5] is in fact a relative maximum of the critical curve. The threshold takes place at $Q \sim 1$ (solution S'_0) however the critical value of the homogeneous solution with transverse flow T_0 lies below that for S'_0 .

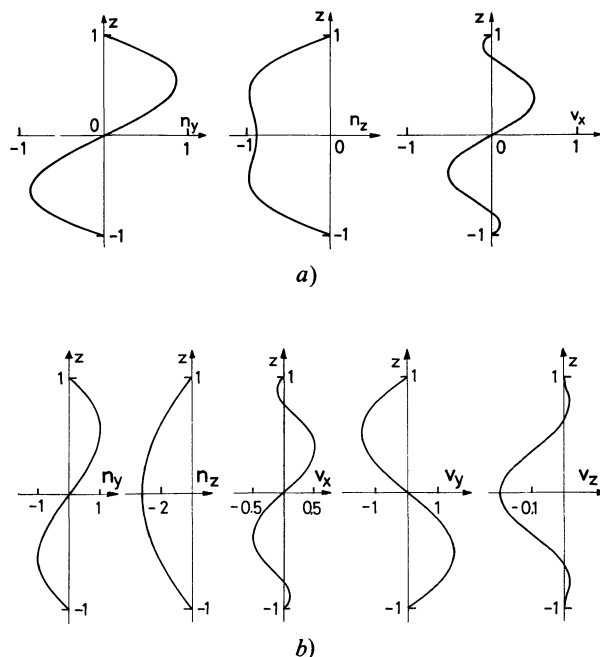


Fig. 11. — Fluctuation profiles for S-type solutions at small wave vectors. The difference between solution S_0 ($Q = 0$, figure 11a) and S'_0 ($Q \sim 1$; figure 11b) is obvious for fluctuation n_z which looks like $\cos(\pi z/d)$ for S'_0 while n_y and v_x bear nearly no change. The contribution of v_y is not negligible when $Q \sim 1$ and should be taken into account in the discussion of the mechanism for S'_0 .

for slightly larger α_3 ($\alpha_3/\alpha_2 \gtrsim 4 \times 10^{-2}$) ⁽³⁾ S'_0 tends towards S_0 which becomes a true minimum instead of being an unstable relative maximum.

As can be seen in figure 10, S'_0 remains above T_0 so that the homogeneous T-instability with transverse flow is expected at threshold in agreement with experiments [4, 9]. Now let us recall that in their first series of experiments [4] Pieranski and Guyon have observed in the non-linear regime above the threshold of the T_0 -mode a roll instability of the S-type with a wavelength 2 or 3 times the thickness of the cell which has all the characteristics of our solution S'_0 ($q_x^c \sim \frac{2}{d} \Rightarrow \lambda_c = 2\pi/q_x^c \sim 3d$). When one increases the external fields the critical value for S'_0 and T_0 remain very close to each other. Using Gähwiler's viscosity values one can even predict a cross-over from T_0 to S'_0 which is not observed experimentally. The reason may be that T_0 is observed in a metastable state due to the operating procedure but more probably that temperature or impurity effects lead to a slightly different set of viscoelastic coefficients. Indeed changing α_3/α_2 from 1.53×10^{-2} to 2.5×10^{-2} is sufficient for the mode T_0 to remain the most unstable one. This interpretation is rein-

⁽³⁾ α_3 is not a free parameter since it enters an Onsager relation but as long as α_3 remains small enough one can neglect the effect of its variation on other viscosity coefficients. Calculations have been performed keeping all viscoelastic coefficients constant except α_3 .

forced by the fact that solution S'_0 has not been observed in the second series of experiments [9], indicating slightly different experimental conditions.

The great sensitivity of the result to the exact value of α_3 has led us to reexamine the instability mechanism of this particular solution S'_0 . Let us assume a long wavelength distortion n_z extending over the whole thickness of the channel (see Fig. 11b)

$$n_z \sim \cos(\pi z/d) \times \cos(q_x x) \quad (q_x \ll 2\pi/d);$$

such a distortion induces a viscous torque [2, 7]

$$\Gamma_z^v = \alpha_2 s n_z$$

which tends to make the director rotate so that a fluctuation n_y appears. When $q_x = 0$ one recovers the original Pieranski-Guyon mechanism for a homogeneous instability [2] corrected to take secondary flow effects into account [7]; namely, viscous forces induce a transverse flow v_x which adds its contribution $-\alpha_3 \partial_z v_x$ to the viscous torque created by the fluctuation n_y ,

$$\Gamma_y^v = -\alpha_3 \partial_z v_x - \alpha_3 s n_y$$

when α_3 is negative this tends to increase the distortion n_z . Now when $q_x \neq 0$, due to the continuity of the fluid, the fluctuation v_x induces a vertical velocity v_z which contributes to the torque Γ_y through a term $-\alpha_2 \partial_x v_z$ ($\alpha_2 < 0$). A careful examination of the global effect shows that the sequence sketched below

$$n_z \xrightarrow{\text{visc. torque}} n_y \xrightarrow{\text{visc. force}} v_x \xrightarrow{\text{continuity}} v_z \xrightarrow{\text{visc. torque}} n_z$$

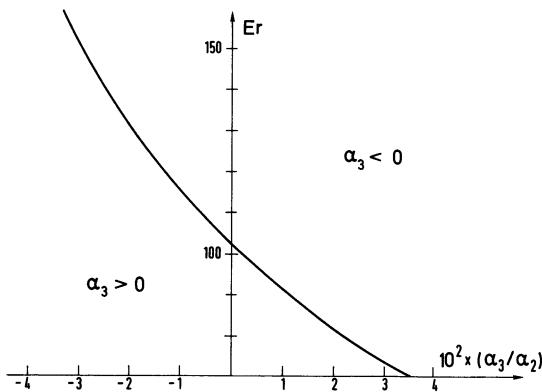


Fig. 12. — Threshold of S'_0 as a function of α_3 . Here

$$Er = \frac{|G_y|}{\eta_3} \left(\frac{d}{2} \right)^3 \frac{|\alpha_2|}{\sqrt{K_1 K_2}}.$$

α_3 is negative at high temperatures and may be positive below some inversion temperature while α_2 remains negative. Notice that a roll instability T_r can also exist, the threshold of which is not much affected by α_3 so that one could witness the cross-over from S'_0 to T_r at another temperature somewhat below the inversion temperature. Calculations have not been performed since detailed viscoelastic data are not available.

works in a destabilizing way as long as $q_x \neq 0$ and small, whatever the value of α_3 positive or negative as long as α_3 is small enough. So when α_3 is positive and small, the usual homogeneous instability T_0 can no longer take place but S'_0 does. Figure 12 displays the threshold of the solution S'_0 for an imaginary nematic which would have the same viscoelastic coefficients as MBBA except for a small and variable α_3 (3). The reduced wave vector $Q = q_x d/2$ slowly varies with α_3 from 0.8 for $\alpha_3 = -2.5 \times 10^{-2} |\alpha_2|$ to 1.2 for $\alpha_3 = +3.3 \times 10^{-2} |\alpha_2|$. The result given above is not of academic interest since there exist nematics for which α_3 varies from negative values close to the clearing point to positive values at lower temperatures, in connection with a tendency to smectic ordering. These nematics will present a cross-over from a solution T_0 to the long wavelength splay distortion S'_0 when the temperature is lowered.

3.3 REMARK : ASYMPTOTIC REGIME FOR ROLLS UNDER HIGH FIELDS. — Despite the fact that rolls are always masked either by a homogeneous instability T_0 or by solution S'_0 , let us consider the asymptotic behaviour of rolls under high fields. It is obtained through an extension of the model of section 2 which combines the idea of unstable layers with results of the simple shear flow instability theory [3] : for rolls, exact results are well accounted for by an *approximate normal mode analysis* which rests on effective torque equations and assumes a simplified analytical form for the fluctuations. Here :

$$n_{y \text{ or } z} \propto \cos(q_z \xi) \cos(q_x x)$$

where ξ is again the distance to the upper and lower plates, and q_z is taken as π/δ , δ being the thickness of the unstable layer submitted to the average shear $\bar{\gamma}(\delta)$. At the limit of high fields and large wave vectors ($q_x^2 \gg q_z^2$) with notations of ref. [3] the critical condition reads

$$\bar{\gamma}^2 \alpha^{*2} \left[1 - 2 \lambda \left(\frac{q_z}{q_x} \right)^2 \right] = [K(q_x^2 + q_z^2) + \chi_a H^2] \quad (4)$$

δ (through q_z and $\bar{\gamma}$) and q_x are two parameters to be optimized, the threshold corresponding to the lowest critical value. With Δ and F as defined in section 2 and

$$Er = \frac{|G_y|}{\eta_3} \left(\frac{d}{2} \right)^3 \frac{\alpha^*}{\bar{K}}, \quad R = (q_x/q_z)^2 \gg 1,$$

eq. (4) reads

$$Er(1 - \Delta/2) = \left(\frac{\pi^2}{\Delta^2} (1 + R) + F \right) / (1 - \lambda/R). \quad (4')$$

Extremum conditions $\partial Er/\partial \Delta = 0$ and $\partial Er/\partial R = 0$ lead to

$$F + 3 \pi^2 (1 + R)/\Delta^2 - 4 \pi^2 (1 + R)/\Delta^3 = 0, \quad (5)$$

$$\frac{\pi^2}{\Delta^2} (1 - \lambda/R) = \left(\frac{\pi^2}{\Delta^2} (1 + R) + R \right) \lambda/R^2. \quad (6)$$

Elimination of F gives

$$R^2 \Delta (1 - \lambda/R) = 2 \lambda (1 + R) (2 - \Delta) \quad (7)$$

which relates the wave vector to the unstable layer thickness. In the limit $R \gg 1$ and $\Delta \ll 1$ this may be simplified to

$$R\Delta = 4\lambda = \text{constant}; \quad (7')$$

the optimum layer thickness is then given by eq. (5)

$$\Delta^4 \sim 16 \pi^2 \lambda/F \quad (5')$$

so that

$$Q_c = q_x^c d/2 = \frac{\pi}{\Delta} \sqrt{R} \sim \Delta^{-3/2} \sim F^{3/8}.$$

As can be seen in figure 13 this asymptotic behaviour is fairly well verified by solution T_r as calculated from the Galerkin expansion. As already stated, the decoupling between the upper and lower half of the channel is more difficult to obtain for S-type rolls, so that agreement with the asymptotic line only appears for the highest calculated points. This fact also explains that threshold values for S_r are about 10 % higher than those for T_r (Fig. 14). Of course such a difference is not accounted for by the simplified model which does not separate solutions of different parities. Finally from (4) and (5') one deduce

$$Er^c = F + o(F^{3/4}) + o(F^{1/2}) + \dots$$

Contrary to the case of the Homogeneous Instability, coefficients entering this expansion are very difficult to estimate and (6) rather gives a general trend of evolution which may help to analyse data

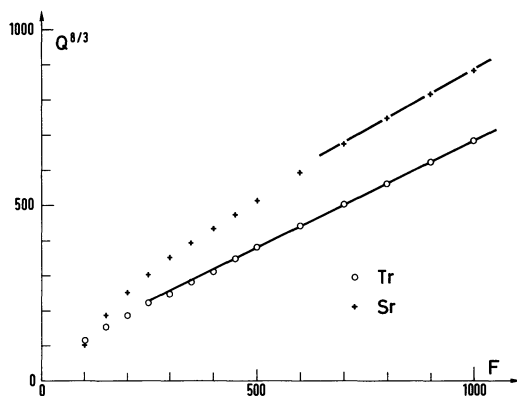


Fig. 13. — An indication of the validity of the approximate model for rolls under large fields is given by the behaviour of the wave vector $Q \sim F^{3/8}$. Dots and crosses correspond to calculated values for T_r and S_r respectively.

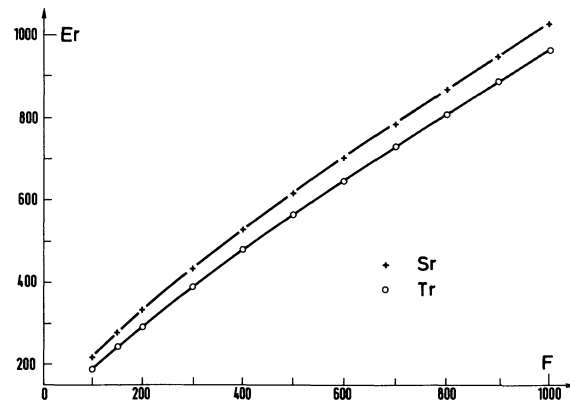


Fig. 14. — The threshold for rolls with average twist (T_r) lies about 10 % below that for rolls with average slay (S_r).

on roll instabilities (see below the alternating flow case).

4. Alternating Poiseuille flows. — From a conceptual point of view it is not difficult to extend the linear stability analysis from the case of a steady flow to that of an alternating one [11]. In the first case one looked for solutions of a differential system with coefficients independent of time under the form $w(\mathbf{r}, t) = w(\mathbf{r}) \exp \sigma t$; marginal stability corresponding to $\text{Re} \{ \sigma \} = 0$ and the exchange of stabilities to $\text{Im} \{ \sigma \} = 0$ at threshold [8]. In the case of a periodic basic flow of period T certain coefficients of the differential system become time-dependent and one cannot eliminate the temporal dependence through a simple exponential factor. As in the case of ordinary differential equations, one assumes a kind of Floquet separation [12]

$$w(\mathbf{r}, t) = \bar{w}(\mathbf{r}, t) \exp \sigma t$$

where \bar{w} is periodic in t with period T . The exponential factor now describes the evolution of the fluctuation once the variation forced by the basic flow has been subtracted. Again the instability sets in when $\text{Re} \{ \sigma \} \geq 0$. Condition $\text{Im} \{ \sigma \} = 0$ at threshold now corresponds to an extension of the hypothesis of *exchange of stabilities*; it merely states that the only period relevant to the problem is the one imposed from the outside. As in the case of steady flows the validity of this assumption should be checked rather than taken for granted. The separation of the temporal dependence in two parts is particularly clear on figure 15 to be discussed further.

The next step is to search for periodic solutions \bar{w} of the eigenvalue problem. At least formally this can be performed through a Fourier expansion :

$$\begin{aligned} \bar{w}(\mathbf{r}, t) = & \frac{1}{2} w_0^c(\mathbf{r}) + \\ & + \sum_{n=1}^{\infty} w_n^c(\mathbf{r}) \cos \left(2 \pi n \frac{t}{T} \right) + w_n^s(\mathbf{r}) \sin \left(2 \pi n \frac{t}{T} \right). \end{aligned}$$

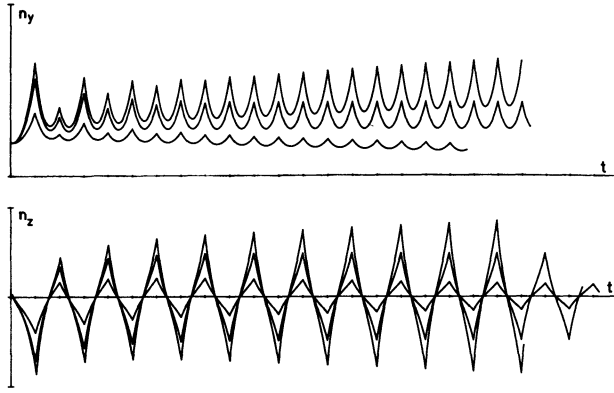


Fig. 15. — Time evolution for the numerical solution of the Homogeneous Instability in square wave alternating flows. Ticks on the time axis mark every reversal of the flow direction (reduced frequency $1/T = (\gamma_1 d^2/4 K_1) f = 12.5$). The upper (resp. lower) curves display the behaviour of n_y (resp. n_z). The 3 or 4 first periods correspond to an adjustment of the spatial profiles of n_y and n_z from those given as initial conditions. Then an asymptotic regime is reached where fluctuations grow ($Er = 130 > Er^c$) or decay ($Er = 90 < Er^c$). We present the case of the Z-regime where n_z changes sign from one 1/2-period to the next. In the marginal case $Er = Er^c \simeq 120$, the exponential trend disappears and one is left with $n_z(t + T/2) = -n_z(t)$ and n_y periodic with period $T/2$.

Time dependent coefficients of the equations are also expanded and after separation of the different harmonics one gets an infinite system of equations where time is absent. Of course the solution is obtained after truncation at a sufficiently high order but from a practical point of view this program is hardly achievable and one is lead to severe approximations. Before entering into details, let us point out the temporal symmetry properties linked to the periodicity of the basic flow. In experiments square wave excitation has been used which is such that

$$s(t + T/2) = -s(t).$$

This allows to distinguish a Z-mode (nomenclature of ref. [2]) where n_z alternates from one half-period to the next ($n_z(t + T/2) = -n_z(t)$) while n_y does not ($n_y(t + T/2) = n_y(t)$) from a Y-mode where n_y and n_z exchange their role. Moreover the fluctuation with the shortest natural relaxation time is expected to oscillate. Classification of the unstable modes in the Poiseuille problem then involves parity and periodicity and one can expect four different regimes Y-T, Z-T, Y-S, Z-S.

4.1 HOMOGENEOUS INSTABILITY. — The homogeneous instability takes place at low frequencies. Even if the equations are much simpler in that case than for rolls, the system has variable coefficients in space and time and the Galerkin procedure has to be performed on both variables. Moreover at low frequencies the exact form of the excitation square wave or sinusoid is important and many

harmonics must be retained (for a discussion in the simple shear flow case see ref. [6]). Several approximations have been worked out leading to unreliable results due to a truncation at a too low order ; this has led us to a frontal attack of the problem, i.e. : to a numerical integration of the *initial and boundary value problem*. In order to compare with experimental results, we shall restrict to the Z-T mode with a square wave excitation in absence of external fields. In that case equations are particularly simple ; in dimensionless form they read [5-7]

$$(1 - \varepsilon) \frac{\partial n_z}{\partial t} = \frac{\partial^2 n_z}{\partial z^2} - Er(t) z n_y$$

$$k \frac{\partial n_y}{\partial t} = \frac{\partial^2 n_y}{\partial z^2} - Er(t) z n_z$$

where $k = K_1/K_2 \sim 2$ and

$$\varepsilon = \alpha_3^2/\gamma_1 \eta_1 \ll 1 \quad (8 \times 10^{-4} \text{ for MBBA}) ;$$

the length scale is $d/2$ and the time scale is given by $4 K_1/\gamma_1 d^2$. Boundary conditions are

$$n_y(z = \pm 1) = n_z(z = \pm 1) = 0.$$

$Er(t) = +E$ over one half-period and $-E$ over the following one.

The most straightforward explicit finite difference scheme [13] turned out to be quite efficient and calculations have been performed with a desk computer. At $t = 0$ we fix approximate profiles for $n_y(z)$ and $n_z(z)$ which fulfil the parity and boundary requirement and we let the solution evolve. On figure 15 one clearly distinguishes a transient regime which corresponds to the adjustment of the spatial dependences from an asymptotic regime of growth, decay or marginal stability according to the value of the Ericksen number. Figure 16 displays

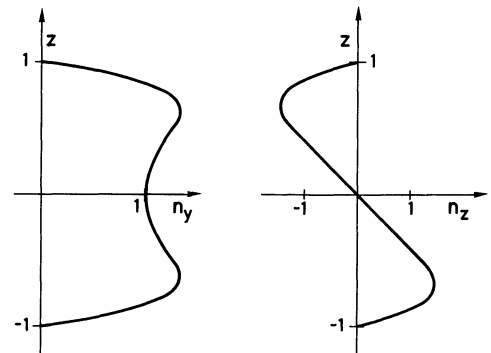


Fig. 16. — Fluctuation profiles at the end of a 1/2-period for $1/T = 12.5$. They look very similar to those for $F \sim 10$ in the steady flow case (see ref. [5]). This could be expected from an analogy between field effects and frequency effects [3]. However this analogy does not work in detail ; in particular to explain the cross-over from uniform distortions to rolls which takes place at a rather low frequency without equivalent in the field case.

the fluctuation profile at the end of a half-period for the highest frequency examined. As in the case of steady flows under magnetic field, one witnesses the constitution of a stable sheet between two unstable layers. Intuitively this comes from the fact that at sufficiently high frequency the instability has not enough time to develop over a large distance from the plate before the flow direction is reversed. However a simple model analogous to that of section 2 shows that the unstable layer thickness δ varies as $T^{2/5}$ and that $Er \sim T^{-1} + o(T^{-3/5})$. Finally figure 17 presents the comparison between calculated and experimental values. Experimental points have been scaled using

$$Er = 56 \Delta p \text{ (cm/H}_2\text{O)}$$

$$1/T = 113 f \text{ (s}^{-1}\text{)}$$

to be compared with the corresponding values $Er \simeq 66 \Delta p$ and $1/T \simeq 130 f$ deduced from data compiled in ref. [10].

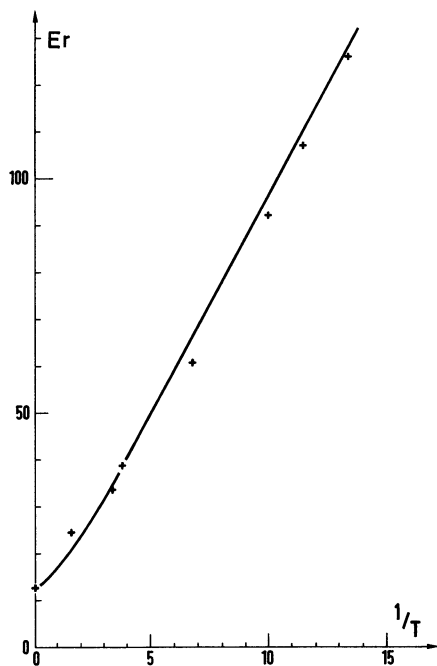


Fig. 17. — Threshold of the Homogeneous Instability in alternating flows. Agreement between the calculated curve and experimental points taken from ref. [9] is very good in view of the somewhat poor precision with which viscoelastic coefficients are known.

4.2 ROLL INSTABILITY MODES. — In addition to the homogeneous mode, roll instabilities have also been observed in the case of alternating flow, in contrast to the case of steady flows under external fields.

Here we shall not be concerned with the cross-over problem which would require a complete solution but rather consider a special case. Indeed equations governing the roll instability are much more involved than those for the homogeneous instability.

Though still possible a direct numerical integration would be much more complicated and one may consider returning to the Galerkin type of approach. However due to the symmetry properties of the unstable modes one will have to solve 4 different systems of equations corresponding to the 4 possible instability regimes. Even restricted to a first harmonic approximation (valid at high enough frequencies) this leads to a rather tedious program. One is then far from the detailed description of stability diagram and more especially from the cross-over problem. Here we shall only consider a simplified approach in terms of unstable layers of adjustable thickness for a solution ⁽⁴⁾ Y-T. The adaptation of the theory developed for the simple shear case is quite straightforward. At a first harmonic approximation, the critical condition is given by [3] :

$$\bar{\gamma}^2 \alpha^{*2} \left[1 - 2 \lambda \left(\frac{q_z}{q_x} \right)^2 \right] =$$

$$= [K(q_x^2 + q_z^2)]^2 + \left(\frac{2\pi}{T} \right)^2 \gamma^{*2} \left[1 + \mu \left(\frac{q_z}{q_x} \right)^2 \right].$$

(The factor 2π arises from the fact that a sinusoidal excitation has been assumed : this makes no difference at high enough frequencies and this has the advantage of leading to a simpler formula than for a square wave excitation [3].) As in § 3.3 one has to adjust the thickness δ of the unstable layer and the wave vector q_x of the rolls. One obtains here

$$\delta \sim T^{2/7} \quad q_x^c \sim T^{-3/7}.$$

Agreement obtained for solution T_r in the steady case gives some confidence in these exotic powers. For the threshold value, they lead to

$$(\Delta p_c)^2 \sim T^{-2} + \theta(T^{-12/7})$$

so that except at rather extreme frequencies one does not expect large departures from the linear dependence of Δp_c with the frequency obtained assuming $\delta \sim 1/q_x \sim T^{1/2}$ [4]. However an experimental check of this asymptotic regime should be searched for. Extensions of this analysis and more results on the basis of direct numerical integration are not very useful before experiments give new data for a quantitative comparison.

5. Conclusion. — At first sight Poiseuille flow could be visualized as the assemblage of two average simple shear flows in order to understand how

⁽⁴⁾ As in the case of a steady flow under high magnetic field, the model does not distinguish solutions of different parities ; the fact that a T-solution appears at threshold [9] is compatible with the arguments already given in section 3.3. In absence of external field, n_y is expected to have the shortest relaxation time and then to oscillate thus leading to a Y-regime [3].

hydrodynamic instabilities can occur. However to a certain extent the experimental situation turned out to be more complex than what could be expected from the transposition of results obtained in the simple shear case. This paper has been mainly devoted to the account of that surprising diversity which originates from the spatial dependence of the basic shearing rate $s(z) \propto z$. (i) In agreement with experimental results rolls analogous to those which develop in the simple shear case have been shown to have a threshold much higher than that of the homogeneous solution. (ii) In addition we have been able to account for the existence of the second metastable homogeneous regime with average twist and no transverse flow observed above the threshold of the first one associated with net transverse flow. (iii) A modification of the original Pieranski-Guyon instability mechanism leads to a long wavelength roll system with average splay. The threshold of this instability (which was observed in the first series of experiments) strongly depends on the viscoelastic constants and more especially on the ratio α_3/α_2 . This sensitivity (quite sufficient to explain the absence of this solution in the second series of experiments) immediately suggests the performance of experiments with a nematic compound where α_3 is positive and small, a situation which forbids homogeneous regimes but leaves intact the mechanism for this particular instability mode.

The three points mentioned above required quantitative predictions. Reliable results have been obtained using an extension of the Galerkin method developed previously. However calculations are rather long, tedious and expensive, moreover they are nearly untractable in the case of alternating flows. These facts have urged one to develop approximate models. The important point was to take into account the spatial dependence of the shear in a simplified but realistic way. Consideration of fluctuation profiles obtained by *exact* calculations has led to the notion

of unstable layer of *variable* thickness submitted to an average shearing rate, the thickness of the layer being determined by some consistency condition. Comparison with *exact* results gives some confidence in such approximate models at least as long as the upper and lower halves of the channel are decoupled by a *stable sheet*, which is pretty well achieved in the case of average twist rolls. An application has been given for the so-called Y-regime in an alternating Poiseuille flow.

Theoretical analysis of alternating flows is rather difficult from a practical point of view even if it is not so complicated conceptually. Beside the development of approximate models there is another approach which seems worth-while, namely the direct integration of the partial differential set of equations taken as an initial and boundary value problem. This method has given excellent results for the alternating homogeneous instability and one can perhaps think of it for more complex situations.

Of course many points remains to be studied such as the truly quantitative account of rolls in alternating flow (and more especially the cross-over from uniform distortion to rolls, non-linear effects for the Z-regime...) and further experiments have been suggested which require a check so that our paper can by no means be considered as exhaustive. However we think that the kind of approach which has been used, combining experimental results with an analysis of mechanisms, detailed calculations, approximate models and numerical simulation can lead to a rather thorough understanding of physical phenomena which occur in complex systems such as flowing nematic liquid crystals as described by the Ericksen-Leslie hydrodynamic theory.

Acknowledgments. — The author would like to thank E. Dubois-Violette and P. Pieranski for interesting discussion concerning theoretical and experimental aspects of this work.

References

- [1] JENKINS, J. T., *Annu. Rev. Fluid Mech.* **10** (1978) 197.
DUBOIS-VIOLETTE, E. *et al.*, in *Liquid Crystals* supplement 14 to *Solid. State Phys.*, L. Liebert ed. (Academic Press, New York) 1978.
- [2] LESLIE, F. M., in *Adv. Liq. Cryst.* **4** Brown ed. (Academic Press, New York) to appear.
- [3] PIERANSKI, P. and GUYON, E., *Solid State Commun.* **13** (1973) 435, *Phys. Rev. A* **9** (1974) 404.
- [4] DUBOIS-VIOLETTE, E. *et al.*, *J. Méc.* **16** (1977) 733.
- [5] LESLIE, F. M., *J. Phys. D* **9** (1976) 925 and *Mol. Cryst. Liq. Cryst.* **37** (1976) 335.
- [6] GUYON, E. and PIERANSKI, P., *J. Physique Colloq.* **36** (1975) C1-203.
- [7] MANNEVILLE, P. and DUBOIS-VIOLETTE, E., *J. Physique* **37** (1976) 1115.
- [8] MANNEVILLE, P., Ph. D thesis, Univ. Paris-Sud n° 1912 (1977).
- [9] MANNEVILLE, P. and DUBOIS-VIOLETTE, E., *J. Physique* **37** (1976) 285.
- [10] See for example CHANDRASEKHAR, S., *Hydrodynamic and Hydromagnetic stability* (Clarendon Press, Oxford) 1961.
- [11] JANOSSY, I., PIERANSKI, P. and GUYON, E., *J. Physique* **37** (1976) 1105.
- [12] See for example : DE GENNES, P. G., *The Physics of Liquid Crystals* (Clarendon Press, Oxford) 1974.
- [13] A recent review of alternating flow stability has been given by DAVIS, *Annu. Rev. Fluid Mech.* **8** (1976) 57.
- [14] This is similar to the case of electrohydrodynamic instabilities in nematic liquid crystals under alternating electrical fields see :
DUBOIS-VIOLETTE, E., DE GENNES, P. G. and PARODI, O., *J. Physique* **32** (1971) 305.
- [15] RICHTMYER, R. D., MORTON, K. W., *Difference Methods for Initial Value Problems* (Interscience Publisher-Wiley, New York) 1967.